NASA-TM-77016 19830012993

NASA TECHNICAL MEMORANDUM

NASA TM-77016

TURBULENT BOUNDARY LAYER AROUND A GROUP OF OBSTACLES IN THE DIRECTION OF FLOW

I. Nakamura, K. Miyata, Y. Yoshiya, R. Nakahama

Translation of "Nagare hoko tokkigun mawari-no ranryu kyokaiso," Nihon Kikai Gakkai Rombunshu (Japan Society of Mechanical Engineers, Transactions), Vol. 45, No. 400, 1979, pp. 1816-1824.

NATIONAL AERONAUTICS AND SPACE ADMINISTRATION
WASHINGTON, D.C. 20546 JANUARY 1983

STANDARD TITLE PAGE

1. Report No. NASA TM-77016	2. Government Accession No.	3. Recipient's Catalog No.
4. Title and Subtitle TURBULENT BOUNDARY LAYER AROUND A GROUP OF OBSTACLES IN THE DIRECTION OF FLOW		5. Report Date January 1983 6. Performing Organization Code
7. Author(s) I. Nakamura, K. Miyata, Y. Yoshiya, R. Nakahama		8. Performing Organization Report No. 10. Work Unit No.
9. Performing Organization Name and Address Leo Kanner Associates Redwood City, California 94063		11. Contract or Grant No. NASW-3541 13. Type of Report and Period Covered Translation
12. Sponsoring Agency Name and Address National Aeronautics and Space Administration, Washington, D.C. 20546		14. Sponsoring Agency Code

15. Supplementary Notes

Translation of "Nagare hoko tokkigun mawari-no ranryu kyokaiso," Nihon Kikai Gakkai Rombunshu (Japan Society of Mechanical Engineers, Transactions), Vol. 45, No. 400, 1979, pp. 1816-1824.

16. Abstract

Results of the investigation are presented with regard to the mean velocity field, velocity distribution of the two-dimensional flow, wall surface shear stresses and Reynolds stresses measured in a downstream cross section where an interference of boundary layers takes place in a flow around adjacent obstacles arranged on the path of flow; such investigation of a boundary layer in a turbulent flow on the surface of a wall having a group of obstacles on the path of flow has never been conducted before.

17. Key Words (Selected by Author(s))	18. Distribution Statement
	Unclassified-Unlimited

19. Security Classif. (of this report)	20. Security Classif. (of this page)	21. No. of Pages	22.
Unclassified	Unclassified		

TURBULENT BOUNDARY LAYER AROUND A GROUP OF OBSTACLES IN THE DIRECTION OF FLOW

I. Nakamura[x)], K. Miyata[x)],
R. Nakahama[xx)], Y. Yoshiya[xxx)]

1. Introduction

/1816*

In the case similar to that for a rough surface with geometrically two-dimensional elements of roughness when the main flow is shifted exactly 90° in a so-called "rough surface flow," obstacles are oriented in parallel with the flow and, as in rough surface flow, flow lamination zones are not formed. In practice, such wall flow very often takes place in heat exchangers. For example, with the trend to miniaturization of modern electric motors a demand arose for improved methods of heat radiation, and a serious problem may arise on the way to optimization if a casing has the above-mentioned obstacles on its surface.

Because an angle to the flow direction is formed when obstacles are arranged in parallel with the flow, according to the authors' previous investigations [1, 2], a two-dimensional flow is formed in the vicinity of the angle similar to the well-known theory of turbulent flow in a rectangular pipe. Thus, multiple longitudinal turbulent interlayers are formed in the developed turbulent boundary layer and within this layer the case should be considered three-dimensional flow.

The authors are aware of the only work (Liu et al. [3]) relating to the case of flow within a turbulent boundary layer along a surface with a group of obstacles arranged in the direction

---

x) Active member, Engineering Faculty of the University of Nagoya.
xx) Active member, Mitsubishi Jidosha Kogyo Co.
xxx) Active member, Gifu Professional High School
* Numbers in the margin indicate pagination in the foreign text.

of flow, and in this case a so-called burst retardation effect is observed. However, the general behavior within the boundary layer is still unknown. In the present investigation, for the case where the obstacles are relatively high with respect to the thickness of the boundary layer, and with regard to the existence of the above-mentioned two-dimensional flow, the authors studied the influence of these factors on the mean velocity field and the field of turbulence. For this purpose, a wall surface was formed by arranging several rows of prisms with a rectangular cross section on a flat plate. This article presents the results of investigations of relationships between the mean velocity field in the turbulent boundary layer formed in the above-mentioned model, two-dimensional flow velocity components, turbulence and Reynolds stress. Wall surface shear stresses were also mentioned.

Symbols

x: coordinates in the direction of flow from the leading edge;

y: coordinates from the wall surface in a direction perpendicular to the flat plate;

z: coordinates from the center of the measuring plate in a direction perpendicular to x,y;

z": distance from the side wall of a prism;

δ: thickness of the boundary layer;

U,V,W: mean velocities within the boundary layer in x,y,z directions, respectively;

u,v,w: fluctuation velocities in x,y,z directions, respectively;

U_o: main flow velocity;

ν: coefficient of kinematic viscosity;

τ_w: wall surface shear stress.

Other symbols are defined in the text where appropriate.

2. Experimental Installation and Testing Method

An experimental installation for the investigation comprises an open-type boundary layer wind tunnel [1] with a two-dimensional constriction having a contraction ratio of 6.55, and a diffuser of 336 x 1125 mm^2. Symbols and schematic representation of the measuring plate are shown in Figure 1. With a height of 60 mm and width of 20 mm, the length of prisms which comprise an obstacle is equal to 2.1 m. The measuring plate is formed of an aluminum flat plate having on its surface 13 rectangular prisms arranged with 40 mm transverse pitch in the z direction. Therefore, the width of the obstacles and spaces between them are equal. Though it is not shown in the drawing, dull pieces are attached to the front end faces of the prisms, so that their front faces coincide with the leading edge of the flat plate. This prevents the formation of collar vortexes typical for such conditions. Besides, a trip wire of Ø0.8 mm is installed at a distance of 50 mm from the leading edge.

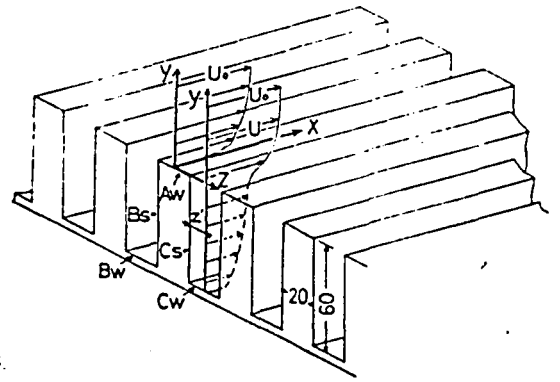

Fig. 1. Configuration of the measuring plate and main symbols.

In the course of the experiments, the measuring plate was attached to a measuring unit provided with a static pressure control gate and a unit Reynolds number U_o/ν was kept constant at the level of 1.40 x 10^6 1/m. Under these conditions, at the main flow velocity of 20-23 m/s the intensity of the turbulence in the main flow was equal to 0.3-0.4%. Measurements were conducted generally in a cross section of x = 1700 mm around the central prism and within the limits of -30 < z < 30 mm. /1817

The Pitot tube and Preston tube used for measuring mean flow velocity and wall surface shear stresses were made of stainless steel in the form of injection needles of 0.6 mm and 1.0 mm outer

diameter, respectively. Furthermore, a two-orifice Pitot tube for measuring the distribution of the two-dimensional flow was installed at a height of 0.5 mm from the leading edge and at a distance of about 1 mm from the center of the pressure inlet, the pressure inlet orifice being arranged at 45^{o} to the measured velocity component [4]. Two constant temperature hot-wire anemometers of standard commercial type and I-type and X-type probes were utilized for measuring Reynolds shear stresses. The probes work automatically.

The wire for the X-type probe comprised a Ø 5 μm tungsten wire with a working part of 1 mm and aspect ratio of 200. A small angle between two wires was measured by means of a universal projector. In the same vision field a reference wire was installed, this reference wire being connected to a microscopic rotary motion device with a minimum readable scale factor of 1'. The main flow coincides with the bisector of said small angle. By means of linear adjustment of the respective anemometers and by means of their gain control, it was possible to perform an analogous treatment of respective signals from the anemometers through automatically adjustable multiplying circuits, and thus to determine Reynolds stresses $-\overline{uv}$, $-\overline{v^2}$. The same procedure was used for determining $\overline{uw}$, $-\overline{w^2}$ after rotating the probes 90^{o} about their axes.

3. Results of Experiments and Their Analysis

3.1. Mean Velocity Field and Two-Dimensional Flow

Figure 2(a), (b) illustrates examples of mean velocity distributions in the direction of the main flow within boundary layers taking place, respectively, on upper surfaces of the prisms and between the prisms. On the upper surface of prisms the velocity distribution in the middle differs very little from the case of a single prism of the same dimensions, and only near the wall surface is an increase of velocity essential. However, the

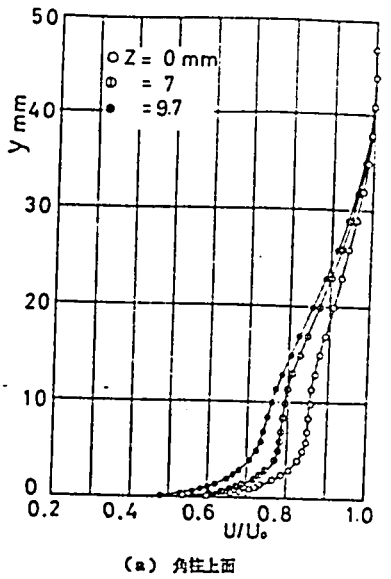

(a) on upper surfaces of prisms

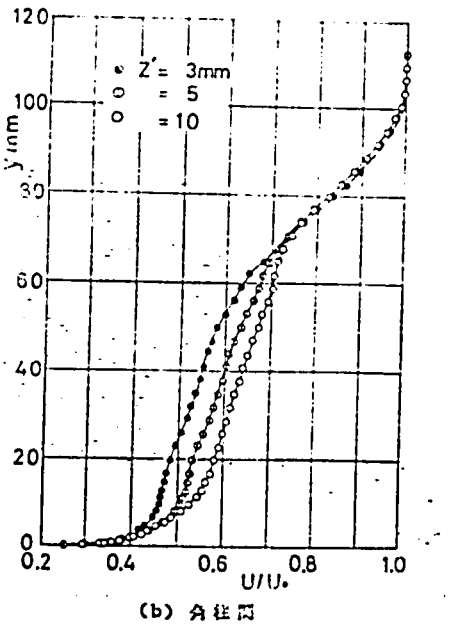

(b) between prisms

Fig. 2. Mean velocity distribution

phase difference is substantial also near the end faces under the effect of adjacent prisms, whereby a three-dimensional turbulence occurs in the vicinity of the wall surface in these areas. On the other hand, a valley is formed on a curve for the between-prism distribution within the limits of $0 \leqq y \leqq 60$ mm. As shown in the drawing, apart from the case in the vicinity of the lower wall surface, in this range the velocity changes almost linearly in the y direction.

Figure 3 shows equal velocity lines in a flow around the central prism, the lines being calculated on the basis of results in Figure 2. As shown in the drawing, contrary to expectation, the /1818
boundary layer has cavities over the obstacles and protrusions over the spaces. As will be explained later, this is an effect of the two-dimensional flow. In the beginning, the boundary layers around adjacent prisms in the upstream flow are formed similarly to that around a single prism, and if an interference of adjacent boundary layers is evaluated on the basis of equal velocity lines [2] for the case of a single prism, it starts from

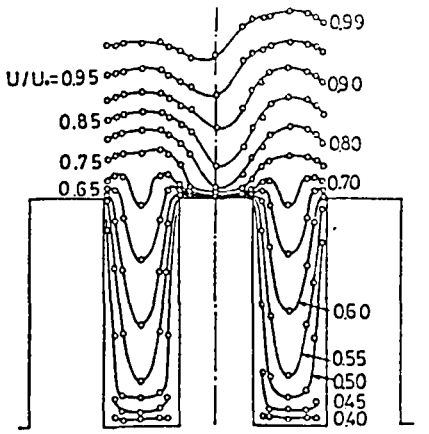

Fig. 3. Equal velocity lines.

the edge in an upwardly inclined direction. Therefore, in the cross sectional area of initial interference a residual potential core zone is formed in between-prism spaces, and this model differs from the flow in an upstream cross section. When the interference is accomplished, the above-mentioned equal velocity lines, which are expanded in the areas, are formed.

A distortion of the equal velocity lines over the prisms is essential and, except in the area in the vicinity of the wall, velocity gradients $\partial v/\partial y$ and $\partial u/\partial z$ are of the same order. On the other hand, spaces accommodate fluid of a relatively low velocity and in this case, equal velocity lines are similar to those in a rectangular shaped pipe. However, as has been mentioned above, $\partial u/\partial y$ in the y direction are almost constant, which fact will later be described as a distinguishing feature of a turbulent flow structure.

Figure 4(a) is a vector representation of two-dimensional flow velocity components V,W, obtained with the use of 2 two-orifice Pitot tubes designed specially for measuring velocity components in the y and z directions. Velocity components V and W can be determined also by means of the above-mentioned X-type probe. However, in this experiment, because of intensive fluctuations, it was extremely difficult to read out the data. Therefore, V and W in the present investigation were measured only by means of the two-orifice Pitot tube. Because of inaccuracy in the results of measurements in the vicinity of wall surfaces having large velocity gradients (in view of the 1 mm distance to the pressure inlet orifice in the two-orifice Pitot tube), these data were omitted.

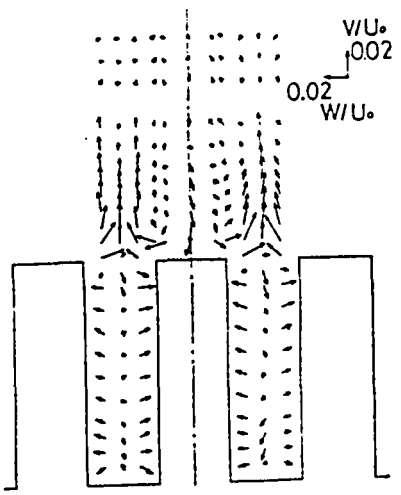

(a) 二次流れ速度のベクトル表示

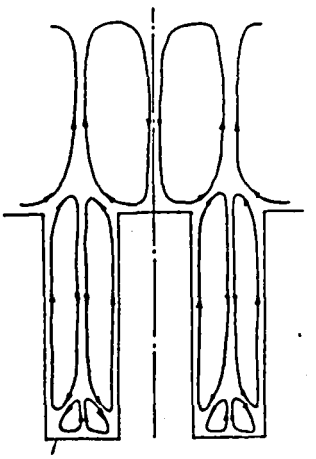

(b) 二次流れのフローパターン

(a) vector representation of two-dimensional flow velocities.

(b) pattern of two-dimensional flow.

Fig. 4. Two-dimensional flow field.

As one could expect from analysis of equal velocity lines on Figure 3, in the area of $y \geq 60$ mm, the two-dimensional flow is directed toward the main flow, whereas on the surface of prisms the flow is directed toward the wall surface. On the other hand, in space areas of $y \geq 60$ mm, in the middle the flow is directed toward the bottom, whereas along the side walls of the prisms, the flow is directed upward. Near edges of prisms the two-dimensional flow is very intensive. However, near the center of spaces the maximum intensity value corresponds to 2.4%. Figure 4(b) illustrates patterns of two-dimensional flows drawn on the basis of Figure 4(a), and although this drawing does not show results of measurements by means of the two orifice Pitot tube and a distortion of the equal velocity curves, it illustrates also a weak two-dimensional flow near corners of the spaces which can be presumed from a distortion of turbulence intensity curves, which are mentioned below, and from lines of equal Reynolds stresses.

3.2. Self-Preservation Velocity Distribution

The authors have already derived the following formula for a self-preservation velocity distribution in the region of a

symmetry plane outer layer of a flow in the three-dimensional turbulent boundary layer [2]:

$$f_s(\eta)=k_3\int_{\eta}^{\infty}\exp\left[-\left\{k_1\eta_0^2+k_2\int_0^{\eta_0}\int_0^{\eta''}\left(\frac{\partial h}{\partial\zeta}\right)_{\zeta=0}d\eta'd\eta''\right\}\right]d\eta_0 \qquad (1)$$

In the above formula: $f_s(\eta) = (U_0-U)/u_\tau$, $h(\eta,\zeta)=W/u_\tau$, $\eta=y/\delta$, $\zeta=z/\delta$, subscript "s" means "plane of symmetry." Furthermore, the following approximate equation can be suggested for distribution $(\partial h/\partial\zeta)_{\zeta=0}$ of microcoefficients of components W in Eq. (1):

$$(\partial h/\partial\zeta)_{\zeta=0}=C[2\pi(\eta-1)]^2\sin 2\pi(\eta-1) \qquad (2)$$

C in formula (2) comprises a constant which is determined by the flow. Figure 5 shows approximately in functional form the right term of Eq. (2) with C equal to 0.028 determined with the use of the results of measurements by means of the above-mentioned two orifice Pitot tube and graphic differentiation.

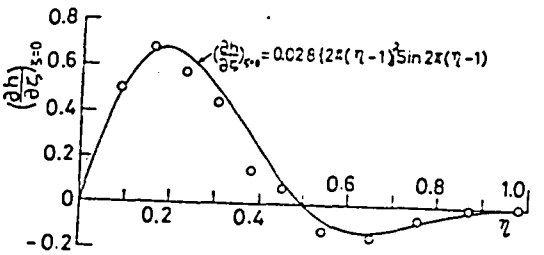

Fig. 5. Distribution of $(\delta h/\delta\zeta)_{\zeta=0}$

The value of C comprises a mean value for the case of a single prism with the same height of 20 mm and width of 60 mm as in the present experiment. Figure 6 illustrates a comparison between the self-preservation velocity distribution function, calculated from Eq. (1) with the use of the above-mentioned value of C, and that obtained experimentally. In the drawing, a solid line represents the case of Eq. (1) calculated with $k_3 = 18$, within the range of $y/\delta > 0.4$, the curve almost coinciding with the results of experiments. However, there is disagreement between theoretical and experimental data at $y/\delta \approx 0.4$. As explained further, this point corresponds to the maximum value of the Reynolds stress $-\overline{uv}$, and after this, at lower values of y/δ, the following condition takes

/1819

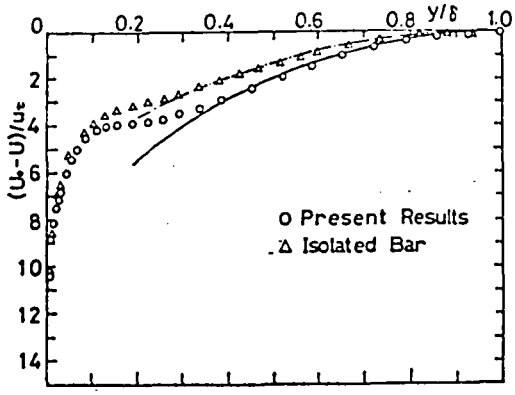

Fig. 6. Self-preservation velocity distribution.

place: $\partial(-\overline{uv})/\partial y > 0$, i.e. $|\partial(-\overline{uv})/\partial y| < |\partial(\overline{uw}/\partial z|$, whereby we cannot neglect the term $\partial(-\overline{uw})/\partial z$ which has been neglected in deriving Eq. (1).

3.3. Wall Surface Shear Stress

The authors have investigated three types of isolated prisms and in all cases mean values of wall surface shear stresses within the area of influence of the prisms were almost the same as for a two-dimensional plate [2]. Therefore, in the present case of multiple arrangement of prisms one can expect that, irrespective of the pitch between the rows, mean wall shear stresses become less than those on the two-dimensional plate. Besides, they have no tendency to increase, on the contrary, they further decrease in proportion to the decrease of the pitch.

In Figure 7 distribution of τ_w, determined by means of the Preston tube, is shown, τ_w being expressed through a dimensionless value $\bar{\tau}_w$. A broken line in this drawing shows results of tests performed by Leutheusser [5] for a rectangular duct with a cross sectional aspect ratio equal to 3. For comparison, a curve designated by circles is given for an isolated prism. As has been anticipated, a mean value of $\bar{\tau}_w$ of wall surface shear stresses for the present experiment is less than that for the isolated prism, and the difference is almost as high as 30%. From this point of view, a friction resistance on the wall surface having a group of obstacles is the same as within the area preceding commencement of interference of boundary layers in the flow around adjacent prisms and corresponds to the value of the resistance on a flat plate having a trip wire. However in the subsequent area, which includes a downstream flow, the resistance is reduced.

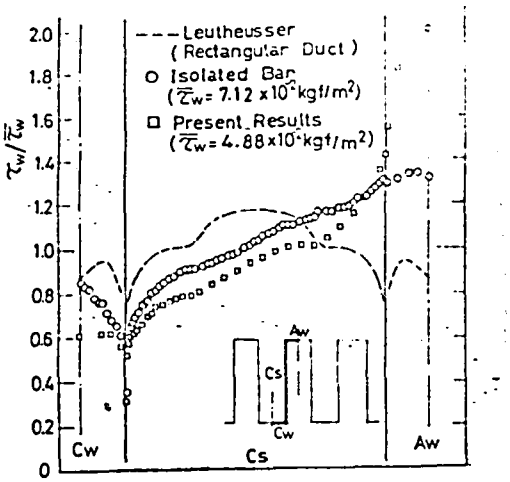

Fig. 7. Distribution of wall surface shear stresses.

As shown in the figure, in the present experiment τ_w has a higher peak on the surface of prisms than in the case of an isolated prism. As can be predicted from the above-mentioned mean velocity distribution on the surface of prisms, this phenomenon is based on the fact that an increase of three-dimensionality results mainly from the impossibility of a two-dimensional flow expanding in a transverse direction further than half pitch because of the existence of adjacent prisms.

3.4 Distribution of Reynolds Stresses

Figure 8 gives a comparison of the results of the present experiment with Klebanoff's case [6]. The results of the present experiment comprise measurements by means of an X-type probe on a smooth flat surface free of a pressure gradient. As shown in the drawing, Reynolds stresses $-\overline{uv}$ almost coincide. However, in the present experiment $\sqrt{\overline{u}^2}$, $\sqrt{\overline{v}^2}$ slightly exceed those of Klebanoff. Nevertheless, the results of measurements by means of the X-type probe may be considered as reliable, at least with regard to $\sqrt{\overline{u}^2}$, because they have rather good coincidence with I-type probe data (black circles in the drawing).

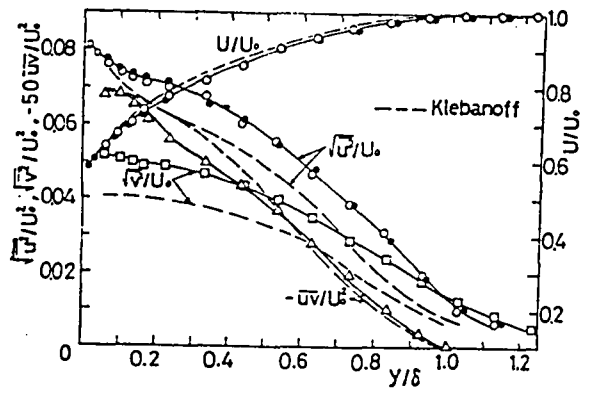

Fig. 8. Distribution of $\sqrt{\overline{u}^2}$, $\sqrt{\overline{v}^2}$, and $-\overline{uv}$ (the flow over a flat plate).

Figure 9(a), (b) shows results of the same measurements at the center on the surface of prisms (z = 0). The results of measurements of U and $\sqrt{\overline{u}^2}$, which correspond to I-type probe measurements, shown by black points, as in the previous drawing, also coincide with those obtained by means of the X-type probe. Because 2 = 0 is a geometrically symmetrical plane, the flow can /1820 also pass symmetrically with respect to this plane. However, as shown in Figure 9(b), the Reynolds stress $-\overline{uw}$ has a relatively large negative value and therefore, strictly speaking, there is not a plane of symmetry with respect to the flow. In reality, the plane $-\overline{uw}$ = 0 is not a z = Constant plane but rather comprises a complicated curvilinear surface. This asymmetry of the flow is also confirmed by means of equal velocity lines in Figure 3. However, until now it has not been clear whether the asymmetry is inherent in the flow which includes multiple turbulent rows formed in the present experiment, or it is a characteristic feature of the experimental installation per se.

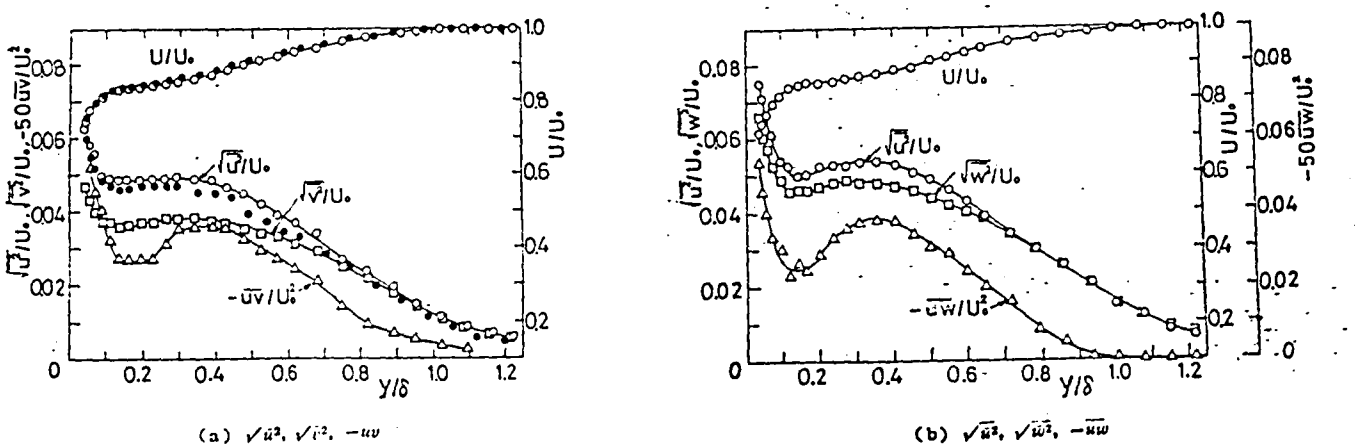

Fig. 9. Distribution of $\sqrt{\overline{u}^2}$, $\sqrt{\overline{v}^2}$, $\sqrt{\overline{w}^2}$, $-\overline{uv}$ and $-\overline{uw}$ (at the center on the surface of prisms).

A distinguishing feature in the case of z = 0 is that Reynolds stresses $-\overline{uv}$ and $-\overline{uw}$ have almost the same absolute values, and both are minimum in the vicinity of the wall surface ($y/\delta \approx 0.2$. At the same time, they have maximum value at $y/\delta \approx 0.4$. From

the point of view of equal velocity lines, $|-\overline{uv}| \simeq |-\overline{uw}|$ in this area correspond to $|\partial u/\partial y| \simeq |\partial u/\partial z|$. A position where the Reynolds stresses are minimum corresponds to that of $\partial y/\partial y \simeq 0$ in the velocity distribution. Therefore, this area is characterized by an extremely small generation of energy in turbulence. Furthermore, because of a very small value of $-\overline{uv}$, in the area of $0.2 < y/\delta < 0.4$ the following condition takes place: $\partial(-uv)/\delta y > 0$. It means that in the case of a two-dimensional flow, fluid elements work with an acceleration. However, in reality, in the same area the following conditions occurs: $|\partial\chi-\overline{uv})/\partial y| < |\partial(\overline{uw})/\partial z|$ and the fluid elements are decelerated. As has been mentioned before, the disagreement between the results of experiments and the self-preservation principle in the velocity distribution starts from the point where Reynolds stresses have the absolute minimum value. From this viewpoint it is clear that $-\overline{uw}$ plays an important role in the analysis.

Figure 10(a), (b) illustrates results of measurements in the middle of spaces, the height of the prisms corresponds to a position with $y/\delta = 0.58$. As shown in the drawing, within the range of $0.1 < y/\delta < 0.5$ the velocity gradient $\partial U/\partial y$ is almost constant. In the same range, the intensity of turbulence $\sqrt{\overline{u^2}}$, $\sqrt{\overline{v^2}}$ $\sqrt{\overline{w^2}}$ is also constant. Besides, all three parameters are almost equal and comprise about 3% of the main flow. On the other hand, contrary to a tendency on the surface of prisms ($\partial u/\partial y \simeq 0$), the value of $-\overline{uv}$ is rather less than that determined from the value of $\sqrt{\overline{v^2}}$, on the basis that $\partial U/\partial y \simeq$ Constant, and it is close to 0.

Figure 11 illustrates by way of example equal turbulence intensity lines only for the case of $\sqrt{\overline{u^2}}$, but for $\sqrt{\overline{v^2}}$ and $\sqrt{\overline{w^2}}$ the distributions have almost the same character. These equal value lines in the vicinity of the outer edge of the boundary /1821
layer are almost parallel to those of Figure 3. Besides, one can see that $\sqrt{\overline{u^2}} \simeq \sqrt{\overline{v^2}} \simeq \sqrt{\overline{w^2}}$. On the other hand, near the edges of prisms with a very strong two-dimensional flow, the equal value lines have a complicated distortion, and, because of an upwardly

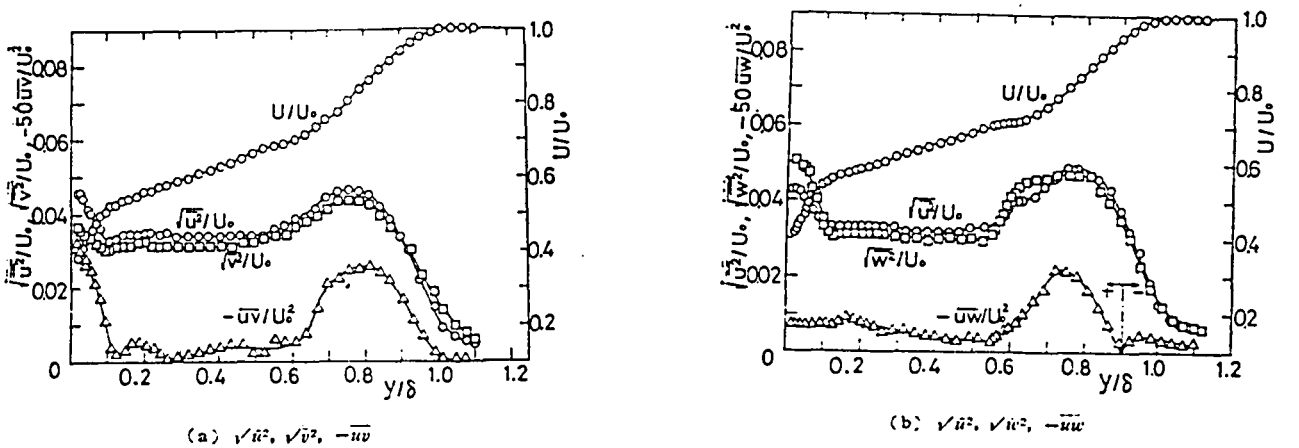

Fig. 10. Distribution of $\sqrt{\overline{u^2}}$, $\sqrt{\overline{v^2}}$, $\sqrt{\overline{w^2}}$, $-\overline{uv}$ and $-\overline{uw}$ (the center of a space between prisms).

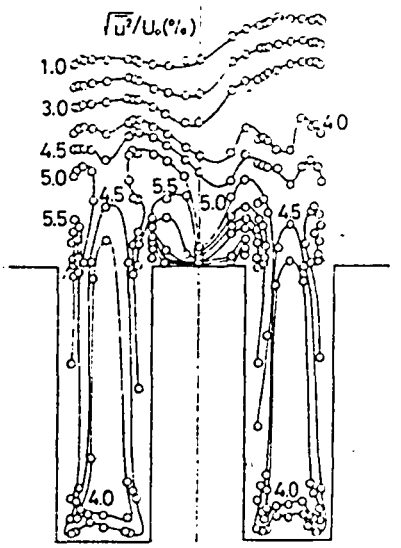

Fig. 11. Equal value lines for $\sqrt{\overline{u^2}}$.

directed two-dimensional flow near the central upper portion of the space, for example as shown by the line of $\sqrt{\overline{u^2}}/U_o$ = 4.5%, equal value lines which are opposite to the direction of the two-dimensional flow have distortions. Although it is not revealed from the analysis of equal value lines of two orifice Pitot tube measurements, some distortions also take place under the effect of a two-dimensional flow near corners of spaces between prisms. Figure 12 illustrates equal value lines of the complete turbulence energy $(\overline{u}^2 + \overline{v}^2 + \overline{w}^2)/2$ expressed through a dimensionless value U_o^2. It is clear that in general the pattern is the same as for $\sqrt{\overline{u^2}}/U_o$ in Figure 11.

The transfer of turbulence energy, quantity of motion (Reynolds shear stresses) and quantity of heat with the turbulent flow

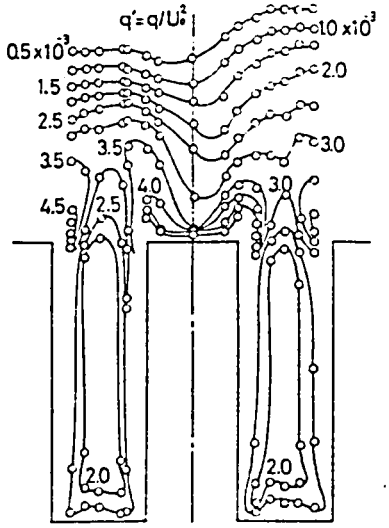

Fig. 12. Equivalent lines of turbulence energy.

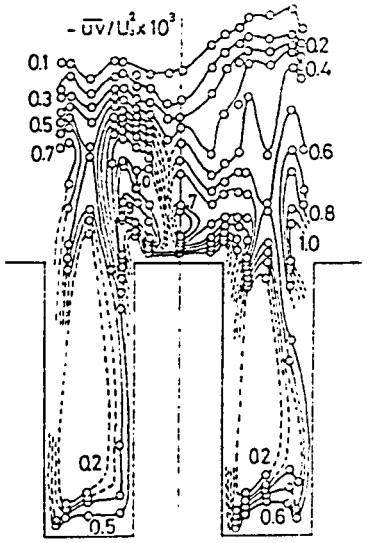

Fig. 13. Equivalent lines of $-\overline{uv}$.

in general is determined as the sum of a small-scale turbulent gradient transfer and counterflow large-scale motion under the effect of the two-dimensional flow which takes place in the present situation. However, in this sum the transfer through the counterflow is dominant with regard to the turbulence energy, as well as the gradient transfer being dominant over the quantity of motion [7]. Figure 13 illustrates equal value lines for Reynolds stresses $-\overline{uv}$. As is obvious from the drawing, these lines have few distinctions from those in Figure 11 and likewise have areas of distortion in the direction opposite the two-dimensional flow. With a gradient character of the transfer of quantity of motion, $-\overline{uv}$ can be expressed through the coefficient ν_τ of turbulent kinematic viscosity in the following manner: /1822

$$-\overline{uv}=\nu_T(\partial U/\partial y+\partial V/\partial x)\fallingdotseq\nu_T\partial U/\partial y. \qquad (3)$$

Here in the area of distortion of equivalent lines of $-\overline{uv}$ in Figure 13, in the direction opposite that of a two-dimensional flow, $\nu U/\nu y$ determined from Figures 2 and 3 in z direction are almost unchanged. Furthermore, because ν_τ locally are substantially constant, it may be assumed that $\nu_\tau \delta U/\partial y\partial z = 0$. On the other hand, because it follows from Fig. 13 that $\partial(-uv)/\partial z \neq 0$, this distortion of curves is consistent with the results of the counterflow transfer of fluid with small values of Reynolds stresses through the upwardly directed

two-dimensional flow. Also the share of the counterflow transfer with respect to $-\overline{uv}$ is rather large even under condition $-\overline{uv} \neq 0$ in the area where, as was disclosed with regard to Figure 9, $\partial U/\partial y$ is approximately equal to 0. Thus, with regard to the transfer of quantity of motion was well, counterflow fluid transfer plays an important role.

3.5. Effect of Energy Balance on Generation of Two-Dimensional Flow.

In the mechanism of generation of the above-described two types of two-dimensional flows, the consideration was based on a momentum equation or an equation of intensity of turbulence. In all these cases the two-dimensional flow is generated under the effect of non-uniformity of vertical Reynolds stresses. With regard to the mechanism of generation of the two-dimensional flow, Gessner [8] suggested the following formula, considering an energy equation of an average flow in the plane of symmetry of flow:

$$(V\rho)\partial P_o/\partial y + \partial(U\overline{uw})/\partial z \approx 0. \qquad (4)$$

wherein $P_o = \rho(U^2 + V^2)/2 + P$. Equation (4) shows the generation of a two-dimensional flow V necessary to compensate for the energy of an average flow lost due to resistance to the Reynolds stresses $-\overline{vw}$.

Figure 14(a), (b) was drawn to study the adaptability of Eq. (4) on the basis of measurements carried out in the present experiment. In Figure 14(a), which illustrates results of measurement at the center on the surface of the prisms, a broken line shows Gessner's results for a rectangular duct. As follows from the drawing, in a major part of the range an accumulation of an average flow energy under the effect of V and energy losses under the effect of $\partial(U\overline{uw})/\partial z$ are almost balanced. Figure 14(b) shows conditions in the middle of the space between prisms, wherein in accordance with the previously described distortion of equal velocity lines and position of reversing the two-dimensional flow

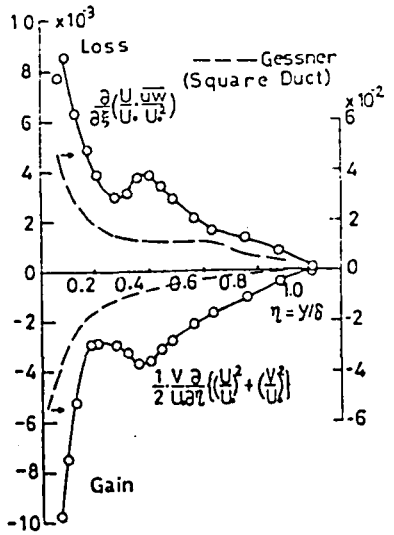

(a) at the center of the prism

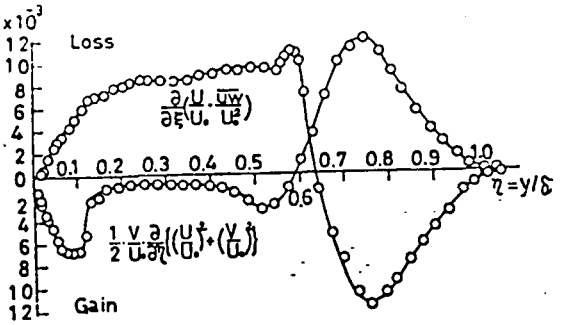

(b) at the center of the space between prisms

Figure 14. Energy balance in an average flow.

almost at the height of the prism, the transformation between the energy loss and energy accumulation can be explained. The balance between losses from V and energy accumulation from $\partial(U\overline{uw})/\partial z$ exists also above the height of the prism. However, in the space between prisms the loss caused by $\partial(U\overline{uw})$ exceeds essentially the accumulation of energy under the effect of V. This fact confirms that for a space between prisms the counterflow term (gain) caused by U should not be neglected. /1823

On the other hand, Hinze [9, 10] suggested the following equation for the mechanism of generation of two-dimensional flow from the viewpoint of the energy balance:

$$V\partial q/\partial y+W\partial q/\partial z+\overline{uv}\partial U/\partial y+\overline{uw}\partial U/\partial z+\varepsilon=0 \qquad (5)$$

wherein $q = (\bar{u}^2 + \bar{v}^2 + \bar{w}^2)/2$ and ε characterizes the viscous dissipation.

Equation (5) characterizes the generation of a two-dimensional flow V,W which determines the supply and removal of turbulent energy on the basis of energy generation and dissipation in the area

where the energy scattering term can be neglected. Because the following condition: $\partial q/\partial y < 0$ occurs generally, when Eq. (5) is applied to the symmetry plane of the flow, it is possible in this case to determine the direction of a two-dimensional flow on the basis of the ratio between the generation and dissipation of energy.

Figure 15 shows the variation of the turbulent energy q on the surface of the prism. A broken line in this drawing relates to Klebanoff's results. As follows from the drawing, q decreases non-monotonously and has its minimum at the point where, under the previously described conditions of $\partial U/\partial y \approx 0$, $-\overline{uv}$ has an extremely small value. This explanation illustrates that, even with the anticipation of the ratio between the energy generation and dissipation, it is not so simple to determine the direction of a two-dimensional flow.

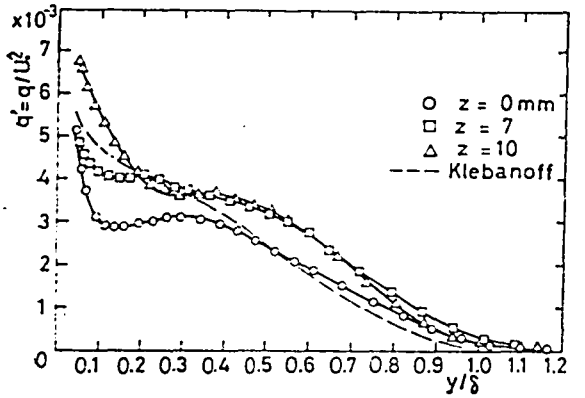

Fig. 15. Distribution of the turbulent energy (on the surface of the prism).

Generally, a turbulence energy equation can be expressed in the following way with respect to a steady three-dimensional flow.

$$U_j\frac{\partial q}{\partial x_j}+\overline{u_iu_j}\frac{\partial U_i}{\partial x_j}+\varepsilon+\frac{\partial}{\partial x_j}\times(q+p'/\rho)u_j-\nu\frac{\partial q}{\partial x_j}-\nu\overline{\frac{\partial u_iu_j}{\partial x_i}}=0 \qquad (6)$$

If the conditions

$$P_1=\overline{uv}\,\partial U/\partial y+\overline{uw}\,\partial U/\partial z$$
$$P_1=\overline{u^2}\,\partial U/\partial x+\overline{v^2}\,\partial V/\partial y+\overline{w^2}\,\partial W/\partial z$$

are taken for the energy generation term $\overline{u_iu_j}\,\partial U_i/\partial x_j$, then 3 terms remaining from the results of the experiments occur one order lower than P_1 and, therefore, can be neglected. Moreover, if we

also neglect the term U∂q/∂x among those for counterflow, the following equation can be derived:

$$V\partial q/\partial y+W\partial q/\partial z+P_s+P_l+\varepsilon+D=0 \quad (7)$$

D in Eq. (7) is an energy scattering term. Figure 16 shows separately each term of the energy distribution Eq. (7), which presents the results of the present experiment. Because in the experiment it was impossible to separate D and ε, they are given as a sum.

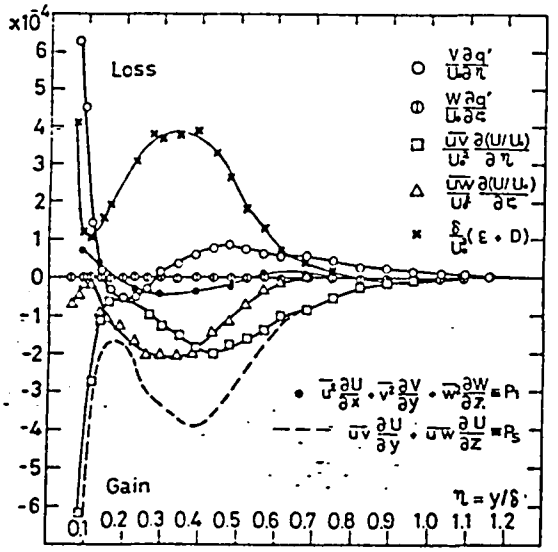

Fig. 16. Turbulence energy balance (in the middle of the surface of the prism).

As shown in the drawing, among the counterflow terms, W∂q/∂z, which is very small within the whole range, can be excluded. However, both terms of P_s are of the same order. The counterflow term V∂q/∂y designates general losses, but due to the above-mentioned monotonous decrease of q in the present experiment, this term appears in the energy accumulation area. Furthermore, the term P_l, which is determined by the aeolotropy of the turbulence, is of the same order as V∂q/∂y. Near the outer edge $\bar{u}^2$, $\bar{v}^2$ and $\bar{w}^2$, which are almost equal, can be neglected.

4. Conclusions

The following conclusions can be drawn with respect to the mean velocity field, velocity of the two-dimensional flow, wall surface shear stresses, and Reynolds stress components, measured in a relatively downstream cross section, where an interference of boundary layers takes place in a flow offluid around adjacent obstacles installed in the path of the flow; such investigation of a boundary layer in a turbulent flow on the surface of a wall /1824

having a group of obstacles arranged on the path of flow has never been conducted before:

(1) Over prismatic obstacles ($y > 60$ mm), a two-dimensional flow on the surface of these obstacles is directed toward wall surfaces, whereas between the obstacles the two-dimensional flow is directed toward the main flow. Therefore, above the obstacles the boundary layer has a valley, and between the obstacles it has a protrusion. A typical two-dimensional flow in a space between obstacles goes downward along a central line of the space and goes upward along both side walls of the space.

(2) An area of a self-preservation velocity distribution function, with constants different from those for a case of an isolated obstacle, appears in the outer layer of flow at the center of the surface of the prisms.

(3) Due to the existence of a low velocity stream in the space between prisms, the mean value of wall surface stresses differs from that for the case of an isolated prism, and it is less than the corresponding value on the surface of a flat two-dimensional plate.

(4) A two-dimensional flow has a pronounced effect on the pattern of Reynolds stress distribution, and in the vicinity of the wall surface at the center on the surface of a prism, the distribution has its minimum. At this point the turbulence energy also has its minimum.

(5) In a relatively large range in the center of the space between prisms a linear velocity distribution takes place in the y direction, which fact suggests that a distinctive mechanism of the turbulent flow generation occurs in this area.

(6) There is no doubt that the conclusion of (4), drawn from the results of the present investigation, was made under

the influence of Hinze's concept with regard to the turbulence energy balance in the generation of a two-dimensional flow. Gessner's energy balance equation also was used.

The authors express their gratitude to those persons and organizations who helped in conducting the present investigations.

REFERENCES

1. Yoshiya et al., Nihon Kikai Gakkai Rombunshu 41/350, 2878 (1975).

2. Yoshiya et al., Nihon Kikai Gakkai Rombunshu 42/359, 2091 (1976).

3. Liu, C. K., Rep. MD-15, Stanford University (1966), 152.

4. Nakamura et al., Proceedings of Japanese Society of Mechanical Engineers 760/15, 21 (1976).

5. Leutheusser, J.J., Trans. Amer. Soc. Civil Engr., HY 3 (1963), 1.

6. Schlichting, H., Boundary Layer Theory, 6th ed., McGraw-Hill, 534, 1968.

7. Hinze, J. O., Turbulence, 2nd ed., McGraw-Hill, 372, 1975.

8. Gessner, F. B., J. Fluid Mech., 58-1, 1 (1973).

9. Hinze, J.O., Phys. Fluids Suppl., 10-2, S 122 (1967).

10. Hinze, J.O., Appl. Sci. Res., 28-6, 453 (1973-12).

End of Document